BPS Dendroscopy on Local Calabi-Yau Threefolds

Boris Pioline

LPTHE LABORATOIRE DE PHYSIQUE THEORIQUE ET HAUTES ENERGIES · cnrs · SORBONNE UNIVERSITÉ

XII Workshop on Geometric Correspondences of Gauge Theories
Zoom@SISSA, 07/07/2022

Work in progress with Pierrick Bousseau, Pierre Descombes and Bruno Le Floch

δενδρον= tree

Dentrology

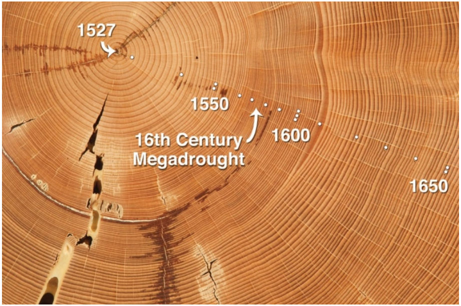

Dendrochronology

δενδροσκοπια= analyzing the BPS spectrum in terms of attractor flow trees

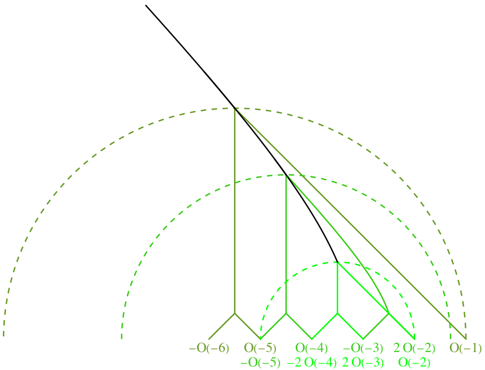

Attractor flow trees, $K_{\mathbb{P}^2}$

$\gamma = [1, 0, -4],\ \mathcal{M} = \mathrm{Hilb}_5\mathbb{P}^2$

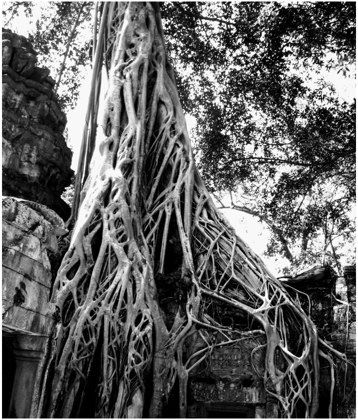

Banyan Tree, Angkor

- In type IIA string theory compactified on a Calabi-Yau threefold X, the BPS spectrum consists of bound states of D6-D4-D2-D0 branes with electromagnetic charge $\gamma \in \Gamma \subset H_{\rm even}(X, \mathbb{Q})$.

Introduction

- In type IIA string theory compactified on a Calabi-Yau threefold X, the BPS spectrum consists of bound states of D6-D4-D2-D0 branes with electromagnetic charge $\gamma \in \Gamma \subset H_{\rm even}(X, \mathbb{Q})$.
- The BPS index $\Omega_z(\gamma)$ counts states with charge γ saturating the BPS bound $M(\gamma) \geq |Z(\gamma)|$, where $Z \in \mathrm{Hom}(\Gamma, \mathbb{C})$ depends on the complexified Kähler moduli $z \in \mathcal{M}$.

Introduction

- In type IIA string theory compactified on a Calabi-Yau threefold X, the BPS spectrum consists of bound states of D6-D4-D2-D0 branes with electromagnetic charge $\gamma \in \Gamma \subset H_{\rm even}(X, \mathbb{Q})$.
- The BPS index $\Omega_z(\gamma)$ counts states with charge γ saturating the BPS bound $M(\gamma) \geq |Z(\gamma)|$, where $Z \in \mathrm{Hom}(\Gamma, \mathbb{C})$ depends on the complexified Kähler moduli $z \in \mathcal{M}$.
- $\Omega_z(\gamma)$ is locally constant on $\mathcal{M}$, but can jump across real codimension one walls of marginal stability $\mathcal{W}(\gamma_1, \gamma_2) \subset \mathcal{M}$, where the phases of the central charges $Z(\gamma_1)$ and $Z(\gamma_2)$ with $\gamma = \gamma_1 + \gamma_2$ become aligned. The jump is governed by a universal wall-crossing formula *[Kontsevich Soibelman'08, Joyce Song'08]*

Introduction

- In type IIA string theory compactified on a Calabi-Yau threefold X, the BPS spectrum consists of bound states of D6-D4-D2-D0 branes with electromagnetic charge $\gamma \in \Gamma \subset H_{\rm even}(X, \mathbb{Q})$.
- The BPS index $\Omega_z(\gamma)$ counts states with charge γ saturating the BPS bound $M(\gamma) \geq |Z(\gamma)|$, where $Z \in \mathrm{Hom}(\Gamma, \mathbb{C})$ depends on the complexified Kähler moduli $z \in \mathcal{M}$.
- $\Omega_z(\gamma)$ is locally constant on $\mathcal{M}$, but can jump across real codimension one walls of marginal stability $\mathcal{W}(\gamma_1, \gamma_2) \subset \mathcal{M}$, where the phases of the central charges $Z(\gamma_1)$ and $Z(\gamma_2)$ with $\gamma = \gamma_1 + \gamma_2$ become aligned. The jump is governed by a universal wall-crossing formula *[Kontsevich Soibelman'08, Joyce Song'08]*
- Physically, multi-centered black hole solutions (dis)appear across the wall *[Denef Moore '07, Manschot BP Sen '11]*. In contrast, single-centered black holes do not decay.

DT invariants and Bridgeland stability conditions

- Mathematically, $\Omega_z(\gamma)$ are generalized Donadson-Thomas invariants for the derived category of coherent sheaves $\mathcal{C} = D^b\mathrm{Coh}(X)$. *[Douglas 2010]*

DT invariants and Bridgeland stability conditions

- Mathematically, $\Omega_z(\gamma)$ are generalized Donadson-Thomas invariants for the derived category of coherent sheaves $\mathcal{C} = D^b\mathrm{Coh}(X)$. *[Douglas 2010]*
- They depend on a choice of Bridgeland stability condition $\sigma = (Z, \mathcal{A})$, where Z is the central charge function and $\mathcal{A}$ a suitable Abelian subcategory of $\mathcal{C}$ such that $\mathrm{Im} Z(\gamma) \geq 0$ for all objects in $\mathcal{A}$ (and $\mathrm{Re} Z(\gamma) < 0$ if $\mathrm{Im} Z(\gamma) = 0$).

DT invariants and Bridgeland stability conditions

- Mathematically, $\Omega_z(\gamma)$ are generalized Donadson-Thomas invariants for the derived category of coherent sheaves $\mathcal{C} = D^b\mathrm{Coh}(X)$. *[Douglas 2010]*
- They depend on a choice of Bridgeland stability condition $\sigma = (Z, \mathcal{A})$, where Z is the central charge function and $\mathcal{A}$ a suitable Abelian subcategory of $\mathcal{C}$ such that $\mathrm{Im}Z(\gamma) \geq 0$ for all objects in $\mathcal{A}$ (and $\mathrm{Re}Z(\gamma) < 0$ if $\mathrm{Im}Z(\gamma) = 0$).
- The space $\mathrm{Stab}(\mathcal{C})$ of Bridgeland stability conditions has complex dimension $b_{even}(X)$. The image of the embedding $\mathcal{M} \hookrightarrow \mathrm{Stab}(\mathcal{C})$ defines the physical slice of Π-stability conditions, of complex codimension $b_{even}(X) - b_2(X) = 1 + b_4(X) + b_6(X)$.

DT invariants and Bridgeland stability conditions

- Mathematically, $\Omega_z(\gamma)$ are generalized Donadson-Thomas invariants for the derived category of coherent sheaves $\mathcal{C} = D^b\mathrm{Coh}(X)$. *[Douglas 2010]*
- They depend on a choice of Bridgeland stability condition $\sigma = (Z, \mathcal{A})$, where Z is the central charge function and $\mathcal{A}$ a suitable Abelian subcategory of $\mathcal{C}$ such that $\mathrm{Im} Z(\gamma) \geq 0$ for all objects in $\mathcal{A}$ (and $\mathrm{Re} Z(\gamma) < 0$ if $\mathrm{Im} Z(\gamma) = 0$).
- The space $\mathrm{Stab}(\mathcal{C})$ of Bridgeland stability conditions has complex dimension $b_{even}(X)$. The image of the embedding $\mathcal{M} \hookrightarrow \mathrm{Stab}(\mathcal{C})$ defines the physical slice of Π-stability conditions, of complex codimension $b_{even}(X) - b_2(X) = 1 + b_4(X) + b_6(X)$.
- There is an action of $\widetilde{GL^+}(2, \mathbb{R})$ on $\mathrm{Stab}(\mathcal{C})$ by rescaling/rotating/stretching Z. This allows to extend Π-stability conditions to a slice of complex codimension $b_4(X) + b_6(X) - 1$.

Bridgeland stability conditions on local surfaces

- For a non-compact CY3 of the form $X = K_S$ where S is a complex Fano surface, the derived category $D^b_c(X)$ of compactly supported coherent sheaves coincides with $D^b\,\mathrm{Coh}(S)$.

Bridgeland stability conditions on local surfaces

- For a non-compact CY3 of the form $X = K_S$ where S is a complex Fano surface, the derived category $D^b_c(X)$ of compactly supported coherent sheaves coincides with $D^b\,\mathrm{Coh}(S)$.
- An object in $D^b\,\mathrm{Coh}(S)$ with Chern vector $\gamma = [r, c_1, \mathrm{ch}_2]$ lifts to a bound state of $Q_4 = r$ D4-branes wrapped on S, $Q_2 \sim c_1$ D2-branes and $Q_0 \sim \mathrm{ch}_2$ D0-branes.

Bridgeland stability conditions on local surfaces

- For a non-compact CY3 of the form $X = K_S$ where S is a complex Fano surface, the derived category $D^b_c(X)$ of compactly supported coherent sheaves coincides with $D^b\,\mathrm{Coh}(S)$.
- An object in $D^b\,\mathrm{Coh}(S)$ with Chern vector $\gamma = [r, c_1, \mathrm{ch}_2]$ lifts to a bound state of $Q_4 = r$ D4-branes wrapped on S, $Q_2 \sim c_1$ D2-branes and $Q_0 \sim \mathrm{ch}_2$ D0-branes.
- At large volume $z^a \to \mathrm{i}\infty$, the central charge for Π-stability is quadratic in $z^a = b^a + \mathrm{i}t^a$,

$$Z(\gamma) \sim -\int_S e^{-z^a H_a}\,\mathrm{ch}\,E = -r\,z^a Q_{ab} z^b + z^a\,\mathrm{ch}_{1,a} - \mathrm{ch}_2$$

  and $\Omega_z(\gamma)$ reduces to the Gieseker index $\Omega_\infty(\gamma)$ counting Gieseker semi-stable sheaves.

Bridgeland stability conditions on local surfaces

- For a non-compact CY3 of the form $X = K_S$ where S is a complex Fano surface, the derived category $D^b_c(X)$ of compactly supported coherent sheaves coincides with $D^b\,\mathrm{Coh}(S)$.
- An object in $D^b\,\mathrm{Coh}(S)$ with Chern vector $\gamma = [r, c_1, \mathrm{ch}_2]$ lifts to a bound state of $Q_4 = r$ D4-branes wrapped on S, $Q_2 \sim c_1$ D2-branes and $Q_0 \sim \mathrm{ch}_2$ D0-branes.
- At large volume $z^a \to \mathrm{i}\infty$, the central charge for Π-stability is quadratic in $z^a = b^a + \mathrm{i}t^a$,

$$Z(\gamma) \sim -\int_S e^{-z^a H_a}\,\mathrm{ch}\,E = -r\,z^a Q_{ab} z^b + z^a\,\mathrm{ch}_{1,a} - \mathrm{ch}_2$$

  and $\Omega_z(\gamma)$ reduces to the Gieseker index $\Omega_\infty(\gamma)$ counting Gieseker semi-stable sheaves.
- Since $b_6(X) = 0$ and $b_4(X) = 1$, subleading corrections to Z can be absorbed by $\widetilde{GL^+}(2,\mathbb{R})$ in a region around large volume.

Dendroscopy on local CY3 manifolds

- Physically, $\Omega_z(\gamma)$ counts BPS states in the 5D-dimensional superconformal field theory engineered by M-theory on X, further reduced along S^1. Macroscopically, they correspond to multi-centered dyon solutions of 4D $\mathcal{N}=2$ effective field theory.

Dendroscopy on local CY3 manifolds

- Physically, $\Omega_z(\gamma)$ counts BPS states in the 5D-dimensional superconformal field theory engineered by M-theory on X, further reduced along S^1. Macroscopically, they correspond to multi-centered dyon solutions of 4D $\mathcal{N}=2$ effective field theory.
- Our goal will be to analyze the BPS spectrum in the simplest case $X = K_{\mathbb{P}^2} = \mathbb{C}^3/\mathbb{Z}_3$, corresponding to a non-Lagrangian SCFT in 5D, and categorize it into various types of multi-centered bound states.

Dendroscopy on local CY3 manifolds

- Physically, $\Omega_z(\gamma)$ counts BPS states in the 5D-dimensional superconformal field theory engineered by M-theory on X, further reduced along S^1. Macroscopically, they correspond to multi-centered dyon solutions of 4D $\mathcal{N}=2$ effective field theory.
- Our goal will be to analyze the BPS spectrum in the simplest case $X = K_{\mathbb{P}^2} = \mathbb{C}^3/\mathbb{Z}_3$, corresponding to a non-Lagrangian SCFT in 5D, and categorize it into various types of multi-centered bound states.
- It will emerge that attractor flow trees for non-compact CY3 are closely connected to scattering diagrams in the space of Bridgeland stability conditions.

Outline

1. Introduction
2. Attractor flow tree formula
3. Quiver scattering diagram
4. Large volume scattering diagram
5. Towards the exact scattering diagram

Outline

Attractor flow and attractor indices

- Recall that for in a spherically symmetric BPS solution of $\mathcal{N} = 2$ supergravity, the Kähler moduli $z^i(r)$ have a radial profile governed by the attractor flow equations

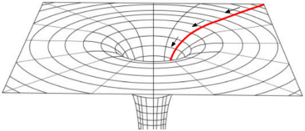

$$r^2 \frac{\mathrm{d}z^i}{\mathrm{d}r} = -g^{i\bar{j}} \partial_{\bar{j}} |Z(\gamma)|^2$$

Ferrara Kallosh Strominger'95

Attractor flow and attractor indices

- Recall that for in a spherically symmetric BPS solution of $\mathcal{N}=2$ supergravity, the Kähler moduli $z^i(r)$ have a radial profile governed by the attractor flow equations

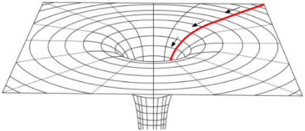

$$r^2 \frac{\mathrm{d}z^i}{\mathrm{d}r} = -g^{i\bar{j}} \partial_{\bar{j}} |Z(\gamma)|^2$$

Ferrara Kallosh Strominger'95

- As $r \to 0$, the moduli reach an attractor point $z_\star(\gamma)$ which minimizes $|Z(\gamma)|$, and is independent of the value at $r=\infty$, at least within a given basin of attraction. The attractor index is defined as the value $\Omega_\star(\gamma) := \Omega_{z_\star(\gamma)}(\gamma)$.

The Attractor Flow Tree formula

- The Attractor Flow Tree Formula postulates that the BPS index $\Omega_z(\gamma)$ at any point $z \in \mathcal{M}$ can be reconstructed from the attractor indices by summing over all possible flow trees: schematically,

$$\Omega_z(\gamma) \sim \sum_{\gamma=\gamma_1+\cdots+\gamma_n} \left(\sum_{T\in\mathcal{T}_z(\{\gamma_i\})} \prod_{v\in V_T} \langle \gamma_{L(v)}, \gamma_{R(v)} \rangle \right) \prod_{i=1}^{n} \Omega_\star(\gamma_i)$$

Denef '00; Denef Greene Raugas '01; Denef Moore'07; Manschot '10, Alexandrov BP'18

The Attractor Flow Tree formula

- The Attractor Flow Tree Formula postulates that the BPS index $\Omega_z(\gamma)$ at any point $z \in \mathcal{M}$ can be reconstructed from the attractor indices by summing over all possible flow trees: schematically,

$$\Omega_z(\gamma) \sim \sum_{\gamma=\gamma_1+\dots+\gamma_n} \left(\sum_{T\in\mathcal{T}_z(\{\gamma_i\})} \prod_{v\in V_T} \langle \gamma_{L(v)}, \gamma_{R(v)} \rangle \right) \prod_{i=1}^{n} \Omega_\star(\gamma_i)$$

Denef '00; Denef Greene Raugas '01; Denef Moore'07; Manschot '10, Alexandrov BP'18

- Here, a flow tree T is a binary rooted tree, with edges decorated with charges γ_e, such that $\gamma_v = \gamma_{L(v)} + \gamma_{R(v)}$ at each vertex, with charges γ_i assigned to the leaves and γ to the root.

The Attractor Flow Tree formula

- The Attractor Flow Tree Formula postulates that the BPS index $\Omega_z(\gamma)$ at any point $z \in \mathcal{M}$ can be reconstructed from the attractor indices by summing over all possible flow trees: schematically,

$$\Omega_z(\gamma) \sim \sum_{\gamma=\gamma_1+\dots+\gamma_n} \left(\sum_{T \in \mathcal{T}_z(\{\gamma_i\})} \prod_{v \in V_T} \langle \gamma_{L(v)}, \gamma_{R(v)} \rangle \right) \prod_{i=1}^{n} \Omega_\star(\gamma_i)$$

Denef '00; Denef Greene Raugas '01; Denef Moore'07; Manschot '10, Alexandrov BP'18

- Here, a flow tree T is a binary rooted tree, with edges decorated with charges γ_e, such that $\gamma_v = \gamma_{L(v)} + \gamma_{R(v)}$ at each vertex, with charges γ_i assigned to the leaves and γ to the root.
- Each edge is embedded in $\mathcal{M}$ along the gradient flow lines of $|Z(\gamma_e)|$, such that the root vertex maps to z, each vertex to $z_v \in \mathcal{W}(\gamma_{L(v)}, \gamma_{R(v)})$, and the leaves to $z_\star(\gamma_i)$.

Split attractor flows

- The physical picture is that typical multi-centered solutions have a nested structure

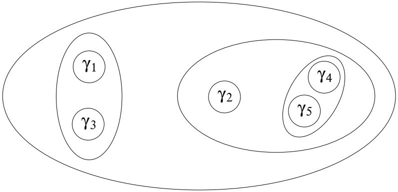

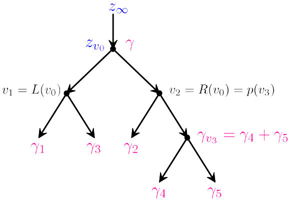

Split attractor flows

- The physical picture is that typical multi-centered solutions have a nested structure

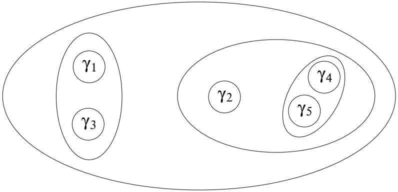

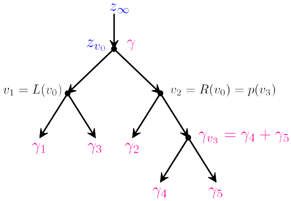

- At each level v, the average distance between the clusters of charge $\gamma_L(v)$ and $\gamma_R(v)$ is fixed, but the orientation in S^2 gives $|\langle \gamma_{L(v)}, \gamma_{R(v)} \rangle|$ degrees of freedom.

Split attractor flows

- The physical picture is that typical multi-centered solutions have a nested structure

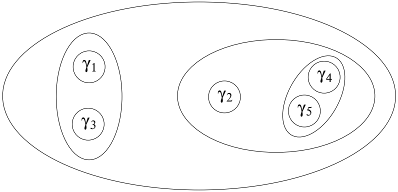

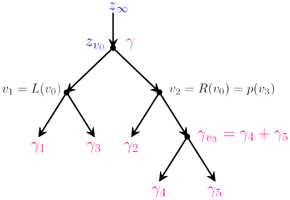

- At each level v, the average distance between the clusters of charge $\gamma_L(v)$ and $\gamma_R(v)$ is fixed, but the orientation in S^2 gives $|\langle \gamma_{L(v)}, \gamma_{R(v)} \rangle|$ degrees of freedom.
- In addition, each center of charge γ_i carries internal degrees of freedom counted by $\Omega_\star(\gamma_i)$.

Remarks

- In order to enforce Bose-Fermi statistics whenever two charges coincide, one should replace $\Omega_z(\gamma)$ by the rational index $\bar{\Omega}_z(\gamma) = \sum_{d|\gamma} \frac{1}{d^2}\Omega_z(\frac{\gamma}{d})$ and insert a Boltzmann symmetry factor. *[Manschot BP Sen'11]*

Remarks

- In order to enforce Bose-Fermi statistics whenever two charges coincide, one should replace $\Omega_z(\gamma)$ by the rational index $\bar{\Omega}_z(\gamma) = \sum_{d|\gamma} \frac{1}{d^2}\Omega_z(\frac{\gamma}{d})$ and insert a Boltzmann symmetry factor. *[Manschot BP Sen'11]*
- When the charges γ_i are not linearly independent, some splittings can involve higher valency vertices. One can treat them using the full KS wall-crossing formula, or perturb the trajectories such that only binary trees remain.

Remarks

- In order to enforce Bose-Fermi statistics whenever two charges coincide, one should replace $\Omega_z(\gamma)$ by the rational index $\bar{\Omega}_z(\gamma) = \sum_{d|\gamma} \frac{1}{d^2}\Omega_z(\frac{\gamma}{d})$ and insert a Boltzmann symmetry factor. *[Manschot BP Sen'11]*
- When the charges γ_i are not linearly independent, some splittings can involve higher valency vertices. One can treat them using the full KS wall-crossing formula, or perturb the trajectories such that only binary trees remain.
- The attractor flow tree formula is consistent with wall-crossing: the index jumps when z crosses the wall $\mathcal{W}(\gamma_{L(v_0)}, \gamma_{R(v_0)})$ associated to the primary splitting for one of the trees.

Remarks

- There are additional ‘fake walls’ where the topology of the trees jump but the total index is constant, thanks to the Jacobi-type identity

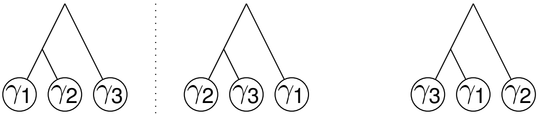

$$\langle\gamma_1,\gamma_2\rangle\,\langle\gamma_1+\gamma_2,\gamma_3\rangle+\text{cyc.}=0$$

Remarks

- There are additional 'fake walls' where the topology of the trees jump but the total index is constant, thanks to the Jacobi-type identity

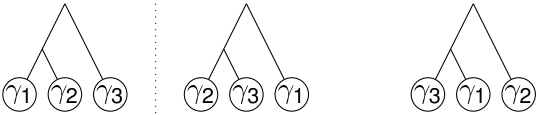

$$\langle\gamma_1,\gamma_2\rangle\,\langle\gamma_1+\gamma_2,\gamma_3\rangle + \text{cyc.} = 0$$

- The formula can be refined by replacing

$$\begin{aligned} \langle\gamma_L,\gamma_R\rangle &\to \frac{y^{\langle\gamma_L,\gamma_R\rangle} - y^{-\langle\gamma_L,\gamma_R\rangle}}{y-1/y} \\ \bar\Omega_z(\gamma) &\to \bar\Omega_z(\gamma,y) = \sum_{d|\gamma} \frac{y-1/y}{d(y^d-y^{-d})}\Omega_z(\tfrac{\gamma}{d},y^d) \end{aligned}$$

Physically, y is a fugacity conjugate to angular momentum in $\mathbb{R}^3$.

Flow tree formula for quivers with potential

- The Attractor Flow Tree Formula can be shown to hold in the context of quiver quantum mechanics: 0+1 dim SUSY gauge theory with $G = \prod_{i \in Q_0} U(N_i)$, bifundamental matter $\Phi_{i\bar{j}}$ for every arrow $(i \to j) \in Q_1$ and superpotential $W = \sum_{w \in Q_2} \lambda_w w$.

Flow tree formula for quivers with potential

- The Attractor Flow Tree Formula can be shown to hold in the context of quiver quantum mechanics: 0+1 dim SUSY gauge theory with $G = \prod_{i\in Q_0} U(N_i)$, bifundamental matter $\Phi_{i\bar{j}}$ for every arrow $(i \to j) \in Q_1$ and superpotential $W = \sum_{w\in Q_2} \lambda_w w$.
- The dimension vector $\gamma = (N_i)_{i\in Q_0}$ plays the role of the charge vector, with Dirac product $\langle\gamma, \gamma'\rangle = \sum_{i\to j}(N_i N'_j - N'_i N_j)$.

Flow tree formula for quivers with potential

- The Attractor Flow Tree Formula can be shown to hold in the context of quiver quantum mechanics: 0+1 dim SUSY gauge theory with $G = \prod_{i \in Q_0} U(N_i)$, bifundamental matter $\Phi_{i\bar{j}}$ for every arrow $(i \to j) \in Q_1$ and superpotential $W = \sum_{w \in Q_2} \lambda_w w$.
- The dimension vector $\gamma = (N_i)_{i \in Q_0}$ plays the role of the charge vector, with Dirac product $\langle \gamma, \gamma' \rangle = \sum_{i \to j} (N_i N'_j - N'_i N_j)$.
- The index $\Omega_\zeta(\gamma)$ is a locally constant function of the Fayet-Iliopoulos parameters $\zeta \in \mathbb{R}^{Q_0}/\mathbb{R}^+$ (aka King stability parameters) with jumps in real codimension 1.

Flow tree formula for quivers with potential

- The Attractor Flow Tree Formula can be shown to hold in the context of quiver quantum mechanics: 0+1 dim SUSY gauge theory with $G = \prod_{i \in Q_0} U(N_i)$, bifundamental matter $\Phi_{i\bar{j}}$ for every arrow $(i \to j) \in Q_1$ and superpotential $W = \sum_{w \in Q_2} \lambda_w w$.
- The dimension vector $\gamma = (N_i)_{i \in Q_0}$ plays the role of the charge vector, with Dirac product $\langle \gamma, \gamma' \rangle = \sum_{i \to j} (N_i N'_j - N'_i N_j)$.
- The index $\Omega_\zeta(\gamma)$ is a locally constant function of the Fayet-Iliopoulos parameters $\zeta \in \mathbb{R}^{Q_0} / \mathbb{R}^+$ (aka King stability parameters) with jumps in real codimension 1.
- For suitable (Q, W) associated to a tilting sequence $(E_1, \dots, E_K)$ on X, there is an isomorphism $D^b_c \mathrm{Coh}(X) \simeq D^b \mathrm{Rep} J(Q, W)$. Near the locus in Stab($\mathcal{C}$) where $Z(\mathrm{ch}\, E_i)$ are nearly aligned, Π- stability reduces to King stability with $\theta_i \propto \mathrm{Im}(e^{-\mathrm{i}\alpha} Z(\gamma_i)]$, $\mathcal{A} = \mathrm{Rep} J(Q, W)$.

Quiver for $K_{\mathbb{P}^2}$

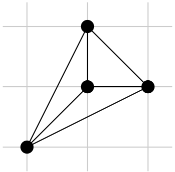

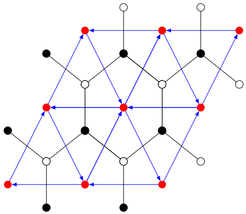

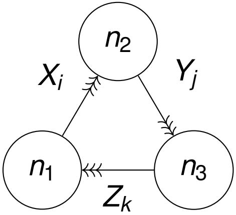

$$W = \sum \epsilon_{ijk} X_i Y_j Z_k$$

$$\begin{aligned} E_1 &= \mathcal{O} & \gamma_1 &= [1,0,0] \\ E_2 &= \Omega(1)[1], & \gamma_2 &= [-2,1,\tfrac{1}{2}] \\ E_3 &= \mathcal{O}(-1)[2] & \gamma_3 &= [1,-1,\tfrac{1}{2}] \end{aligned}$$

$$\begin{aligned} r &= 2n_2 - n_1 - n_3 \\ d &= n_3 - n_2 \\ \mathrm{ch}_2 &= -\tfrac{1}{2}(n_2 + n_3) \end{aligned}$$

Flow tree formula for quivers with potential

- The attractor point becomes the self-stability condition $(\zeta_\star(\gamma),\cdot) = \langle\gamma,\cdot\rangle$. The attractor indices $\Omega_\star(\gamma_i)$ depend on W.

Flow tree formula for quivers with potential

- The attractor point becomes the self-stability condition $(\zeta_\star(\gamma), \cdot) = \langle \gamma, \cdot \rangle$. The attractor indices $\Omega_\star(\gamma_i)$ depend on W.
- The attractor flow becomes linear,

$$(\zeta_v, \cdot) = (\zeta_{p(v)}, \cdot) + \lambda \frac{(\zeta_{p(v)}, \gamma_{L(v)})}{\langle \gamma_{L(v)}, \gamma_{R(v)} \rangle} \langle \gamma_v, \cdot \rangle \,, \quad 0 \leq \lambda \leq 1$$

Manschot'10; Alexandrov BP'18

Flow tree formula for quivers with potential

- The attractor point becomes the self-stability condition $(\zeta_\star(\gamma), \cdot) = \langle \gamma, \cdot \rangle$. The attractor indices $\Omega_\star(\gamma_i)$ depend on W.
- The attractor flow becomes linear,

$$(\zeta_v, \cdot) = (\zeta_{p(v)}, \cdot) + \lambda \frac{(\zeta_{p(v)}, \gamma_{L(v)})}{\langle \gamma_{L(v)}, \gamma_{R(v)} \rangle} \langle \gamma_v, \cdot \rangle , \quad 0 \le \lambda \le 1$$

Manschot'10; Alexandrov BP'18

- Since $N_i \geq 0$, only a finite number of trees contribute. When $N_i > 1$, a small perturbation of ζ is necessary so as to restrict to binary trees.

Flow tree formula for quivers with potential

- The attractor point becomes the self-stability condition $(\zeta_\star(\gamma),\cdot) = \langle\gamma,\cdot\rangle$. The attractor indices $\Omega_\star(\gamma_i)$ depend on W.
- The attractor flow becomes linear,

$$(\zeta_v,\cdot) = (\zeta_{p(v)},\cdot) + \lambda \frac{(\zeta_{p(v)},\gamma_{L(v)})}{\langle\gamma_{L(v)},\gamma_{R(v)}\rangle}\langle\gamma_v,\cdot\rangle\ , \quad 0\leq\lambda\leq 1$$

Manschot'10; Alexandrov BP'18

- Since $N_i \geq 0$, only a finite number of trees contribute. When $N_i > 1$, a small perturbation of ζ is necessary so as to restrict to binary trees.
- The Attractor Flow Tree formula was established rigorously using the framework of scattering diagrams *[Argüz Bousseau '20]*. See *[Mozgovoy'20]* for a proof of another version using operads.

Outline

Flow tree formula from scattering diagrams

- For any quiver with potential (Q, W), the scattering diagram $\mathcal{D}$ is the set of real codimension-one rays $\{\mathcal{R}(\gamma), \gamma \in \mathbb{Z}^{Q_0}\}$ defined by *[Bridgeland'16]*

$$\mathcal{R}(\gamma) = \{\zeta \in \mathbb{R}^{Q_0} : (\zeta, \gamma) = 0, \Omega_\zeta(k\gamma) \neq 0 \text{ for some } k \geq 1\}$$

Flow tree formula from scattering diagrams

- For any quiver with potential (Q, W), the scattering diagram $\mathcal{D}$ is the set of real codimension-one rays $\{\mathcal{R}(\gamma), \gamma \in \mathbb{Z}^{Q_0}\}$ defined by *[Bridgeland'16]*

$$\mathcal{R}(\gamma) = \{\zeta \in \mathbb{R}^{Q_0} : (\zeta, \gamma) = 0, \Omega_\zeta(k\gamma) \neq 0 \text{ for some } k \geq 1\}$$

- Each point along $\mathcal{R}(\gamma)$ is endowed with an automorphism of the quantum torus algebra, (assume γ primitive)

$$\mathcal{U}(\gamma) = \exp(\sum_{m=1}^{\infty} \frac{\bar{\Omega}_\zeta(k\gamma, y)}{y^{-1} - y} \mathcal{X}_{k\gamma}) , \quad \mathcal{X}_\gamma \mathcal{X}_{\gamma'} = (-y)^{\langle \gamma, \gamma' \rangle} \mathcal{X}_{\gamma+\gamma'}$$

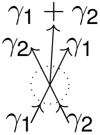

• The WCF ensures that the diagram is consistent, $\prod_{\gamma_i} \mathcal{U}(\gamma_i)^{\pm 1} = 1$ around any codimension 2 intersection. The Attractor Flow Tree Formula determines outgoing rays from incoming rays at each vertex. *[Argüz Bousseau '20]*.

Attractor conjecture for $K_{\mathbb{P}^2}$

- By examining the expected dimension of the moduli space of quiver representations, *[Beaujard BP Manschot'20]* conjectured that all attractor invariants $\Omega_\star(\gamma)$ vanish except

Attractor conjecture for $K_{\mathbb{P}^2}$

- By examining the expected dimension of the moduli space of quiver representations, *[Beaujard BP Manschot'20]* conjectured that all attractor invariants $\Omega_\star(\gamma)$ vanish except
  - $\Omega_\star(\gamma_i) = 1$ for $i = 1, 2, 3$

Attractor conjecture for $K_{\mathbb{P}^2}$

- By examining the expected dimension of the moduli space of quiver representations, *[Beaujard BP Manschot'20]* conjectured that all attractor invariants $\Omega_\star(\gamma)$ vanish except
  - $\Omega_\star(\gamma_i) = 1$ for $i = 1, 2, 3$
  - $\Omega_\star(k(\gamma_1 + \gamma_2 + \gamma_3)) = -y^3 - y - 1/y$ for $k \geq 1$.

Attractor conjecture for $K_{\mathbb{P}^2}$

- By examining the expected dimension of the moduli space of quiver representations, *[Beaujard BP Manschot'20]* conjectured that all attractor invariants $\Omega_\star(\gamma)$ vanish except
  - $\Omega_\star(\gamma_i) = 1$ for $i = 1, 2, 3$
  - $\Omega_\star(k(\gamma_1 + \gamma_2 + \gamma_3)) = -y^3 - y - 1/y$ for $k \geq 1$.
- Under this assumption, we observed that the index $\Omega_{-\zeta_\star(\gamma)}(\gamma)$ for $\gamma = (n_1, n_2, n_3)$, in the anti-attractor chamber coincides with the index $\Omega_\infty(r, d, \mathrm{ch}_2)$ counting Gieseker semi-stable sheaves provided $r > 0$ and $-r \leq d \leq 0$. But the quiver description is only supposed to be valid near the orbifold point !

Attractor conjecture for $K_{\mathbb{P}^2}$

- By examining the expected dimension of the moduli space of quiver representations, *[Beaujard BP Manschot'20]* conjectured that all attractor invariants $\Omega_\star(\gamma)$ vanish except
  - $\Omega_\star(\gamma_i) = 1$ for $i = 1, 2, 3$
  - $\Omega_\star(k(\gamma_1 + \gamma_2 + \gamma_3)) = -y^3 - y - 1/y$ for $k \geq 1$.
- Under this assumption, we observed that the index $\Omega_{-\zeta_\star(\gamma)}(\gamma)$ for $\gamma = (n_1, n_2, n_3)$, in the anti-attractor chamber coincides with the index $\Omega_\infty(r, d, \mathrm{ch}_2)$ counting Gieseker semi-stable sheaves provided $r > 0$ and $-r \leq d \leq 0$. But the quiver description is only supposed to be valid near the orbifold point !
- A similar conjecture for $\Omega_\star(\gamma)$ holds for any toric CY3, giving in principle access to DT invariants $\Omega_\zeta(\gamma)$ for any $\zeta \in \mathbb{R}^{Q_0}$ *[Mozgovoy BP'20; Descombes'21]*

Orbifold scattering diagram

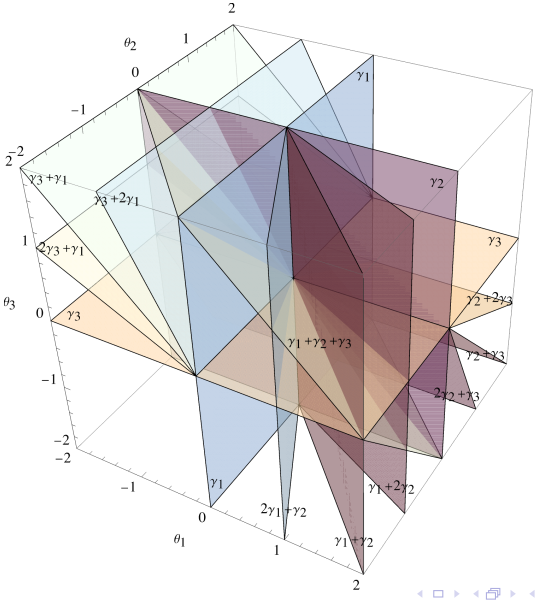

A 2D slice of the orbifold scattering diagram

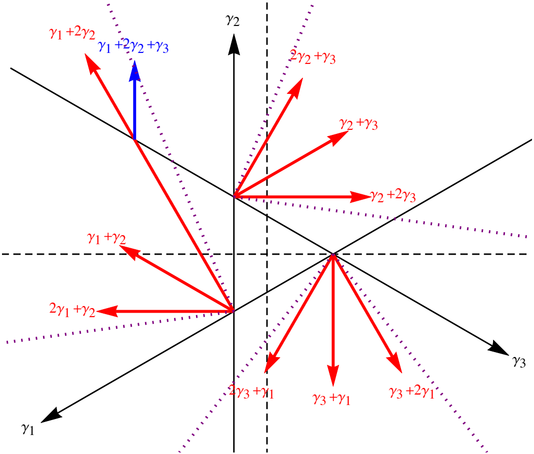

Flow trees from scattering diagrams

- More generally, for any $\psi \in \mathbb{R}/2\pi\mathbb{Z}$ define scattering rays as loci

$$\mathcal{R}_\psi(\gamma) = \{Z : \mathrm{Re}(e^{-\mathrm{i}\psi} Z(\gamma)) = 0, \mathrm{Im}(e^{-\mathrm{i}\psi} Z(\gamma)) > 0, \Omega_\zeta(k\gamma) \neq 0\}$$

Flow trees from scattering diagrams

- More generally, for any $\psi \in \mathbb{R}/2\pi\mathbb{Z}$ define scattering rays as loci

$$\mathcal{R}_\psi(\gamma) = \{Z : \mathrm{Re}(e^{-\mathrm{i}\psi} Z(\gamma)) = 0, \mathrm{Im}(e^{-\mathrm{i}\psi} Z(\gamma)) > 0, \Omega_\zeta(k\gamma) \neq 0\}$$

- For a non-compact CY3, $Z(\gamma)$ is holomorphic in Kähler moduli, thus arg $Z(\gamma)$ is constant along the gradient flow of $|Z(\gamma)|$. Choosing ψ such that $z \in \mathcal{R}_\psi(\gamma)$, edges of attractor flow trees lie inside $\mathcal{R}_\psi(\gamma_e)$, while vertices lie in $\mathcal{R}_\psi(\gamma_{L(v)}) \cap \mathcal{R}_\psi(\gamma_{R(v)})$.

Flow trees from scattering diagrams

- More generally, for any $\psi \in \mathbb{R}/2\pi\mathbb{Z}$ define scattering rays as loci

$$\mathcal{R}_\psi(\gamma) = \{Z : \mathrm{Re}(e^{-\mathrm{i}\psi} Z(\gamma)) = 0, \mathrm{Im}(e^{-\mathrm{i}\psi} Z(\gamma)) > 0, \Omega_\zeta(k\gamma) \neq 0\}$$

- For a non-compact CY3, $Z(\gamma)$ is holomorphic in Kähler moduli, thus $\arg Z(\gamma)$ is constant along the gradient flow of $|Z(\gamma)|$. Choosing ψ such that $z \in \mathcal{R}_\psi(\gamma)$, edges of attractor flow trees lie inside $\mathcal{R}_\psi(\gamma_e)$, while vertices lie in $\mathcal{R}_\psi(\gamma_{L(v)}) \cap \mathcal{R}_\psi(\gamma_{R(v)})$.
- Besides, since $Z(\gamma)$ is holomorphic, initial rays must originate from attractor points on the boundary.

Flow trees from scattering diagrams

- More generally, for any $\psi \in \mathbb{R}/2\pi\mathbb{Z}$ define scattering rays as loci

$$\mathcal{R}_\psi(\gamma) = \{Z : \mathrm{Re}(e^{-\mathrm{i}\psi} Z(\gamma)) = 0, \mathrm{Im}(e^{-\mathrm{i}\psi} Z(\gamma)) > 0, \Omega_\zeta(k\gamma) \neq 0\}$$

- For a non-compact CY3, $Z(\gamma)$ is holomorphic in Kähler moduli, thus arg $Z(\gamma)$ is constant along the gradient flow of $|Z(\gamma)|$. Choosing ψ such that $z \in \mathcal{R}_\psi(\gamma)$, edges of attractor flow trees lie inside $\mathcal{R}_\psi(\gamma_e)$, while vertices lie in $\mathcal{R}_\psi(\gamma_{L(v)}) \cap \mathcal{R}_\psi(\gamma_{R(v)})$.
- Besides, since $Z(\gamma)$ is holomorphic, initial rays must originate from attractor points on the boundary.
- Thus, flow trees are subsets of scattering diagrams, determining sequences of scatterings which produce an outgoing ray $\mathcal{R}_\psi(\gamma)$ passing through the desired point z.

Outline

Kähler moduli space of $K_{\mathbb{P}^2}$

- The Kähler moduli space of $K_{\mathbb{P}^2}$ is the modular curve $X_1(3) = \mathbb{H}/\Gamma_1(3)$ parametrizing elliptic curves with level structure. It admits two cusps LV, C and one elliptic point o of order 3.

Kähler moduli space of $K_{\mathbb{P}^2}$

- The Kähler moduli space of $K_{\mathbb{P}^2}$ is the modular curve $X_1(3) = \mathbb{H}/\Gamma_1(3)$ parametrizing elliptic curves with level structure. It admits two cusps LV, C and one elliptic point o of order 3.
- The universal cover is parametrized by $\tau \in \mathbb{H}$:

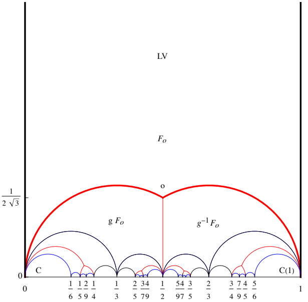

$$
\begin{aligned}
Z_\tau(\gamma) &= -rT_D(\tau) + dT(\tau) - \mathrm{ch}_2 \\
T &= \int_\ell \lambda \\
T_D &= \int_{\ell_D} \lambda
\end{aligned}
$$

λ holomorphic one-form with logarithmic singularities on $\mathcal{E}_\tau$

Central charge as Eichler integral

- Since $\partial_\tau \lambda$ is holomorphic, its periods are proportional to $(1, \tau)$. Integrating on a path from o to τ, one finds the Eichler-type integral

$$\boxed{\begin{pmatrix} T \\ T_D \end{pmatrix} = \begin{pmatrix} 1/2 \\ 1/3 \end{pmatrix} + \int_{\tau_o}^{\tau} \begin{pmatrix} 1 \\ u \end{pmatrix} C(u)\, \mathrm{d}u}$$

where $C(\tau) = \frac{\eta(\tau)^9}{\eta(3\tau)^3}$ is a weight 3 modular form for $\Gamma_1(3)$.

Central charge as Eichler integral

- Since $\partial_\tau \lambda$ is holomorphic, its periods are proportional to $(1, \tau)$. Integrating on a path from o to τ, one finds the Eichler-type integral

$$\boxed{\begin{pmatrix} T \\ T_D \end{pmatrix} = \begin{pmatrix} 1/2 \\ 1/3 \end{pmatrix} + \int_{\tau_o}^{\tau} \begin{pmatrix} 1 \\ u \end{pmatrix} C(u)\,\mathrm{d}u}$$

  where $C(\tau) = \frac{\eta(\tau)^9}{\eta(3\tau)^3}$ is a weight 3 modular form for $\Gamma_1(3)$.

- This provides an computationally efficient analytic continuation of Z_τ throughout $\mathbb{H}$, and gives access to monodromies:

$$\tau \mapsto \frac{a\tau + b}{c\tau + d} \qquad \begin{pmatrix} 1 \\ T \\ T_D \end{pmatrix} \mapsto \begin{pmatrix} 1 & 0 & 0 \\ m & d & c \\ m_D & b & a \end{pmatrix} \cdot \begin{pmatrix} 1 \\ T \\ T_D \end{pmatrix}$$

  where (m, m_D) are period integrals of C from τ_o to $\frac{a\tau_o - b}{c\tau_o - d}$.

Central charge as Eichler integral

- At large volume, using $C = 1 - 9q + \dots$ one finds

$$T = \tau + \mathcal{O}(q), \quad T_D = \frac{1}{2}\tau^2 + \frac{1}{8} + \mathcal{O}(q)$$

Central charge as Eichler integral

- At large volume, using $C = 1 - 9q + \dots$ one finds

$$T = \tau + \mathcal{O}(q), \quad T_D = \frac{1}{2}\tau^2 + \frac{1}{8} + \mathcal{O}(q)$$

- For τ_2 large enough, one can use the $GL(2,\mathbb{R})^+$ action on Stab $\mathcal{C}$ to absorb the $\mathcal{O}(q)$ corrections and work with

$$Z^{LV}_{(s,t)}(\gamma) = -\frac{r}{2}(s+\mathrm{i}t)^2 + d(s+\mathrm{i}t) - \mathrm{ch}_2 \,,$$

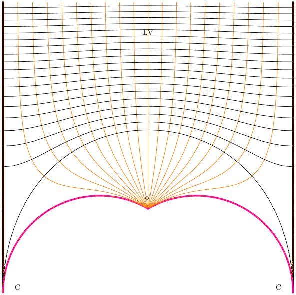

$$s = \frac{\mathrm{Im}\, T_D}{\mathrm{Im}\, T}\,, \quad \mu = \frac{d}{r}$$

$$\frac{1}{2}(s^2+t^2) = -\frac{\mathrm{Im}(T\bar{T}_D)}{\mathrm{Im}\, T}$$

$$\mathcal{A} = \{E \xrightarrow{d} F, \mu(E) < s, \mu(F) \geq s\}$$

Large volume scattering diagram

- For the stability conditions $(Z^{LV_{(s,t)}}, \mathcal{A}(s))$, *[Bousseau'19]* constructed the scattering diagram $\mathcal{D}_\psi$ in (s,t) upper half-plane for $\psi = 0$. For $\psi \neq 0$, just map $(s,t) \mapsto (s - t\tan\psi, t/\cos\psi)$.

Large volume scattering diagram

- For the stability conditions $(Z^{LV_{(s,t)}}, \mathcal{A}(s))$, [Bousseau'19] constructed the scattering diagram $\mathcal{D}_\psi$ in (s,t) upper half-plane for $\psi = 0$. For $\psi \neq 0$, just map $(s,t) \mapsto (s - t\tan\psi, t/\cos\psi)$.
- The rays $\mathcal{R}(\gamma)$ are branches of hyperbola asymptoting to $t = \pm(s - \frac{d}{r})$ for $r \neq 0$, or vertical lines when $r = 0$. Walls of marginal stability $\mathcal{W}(\gamma,\gamma')$ are half-circles centered on real axis.

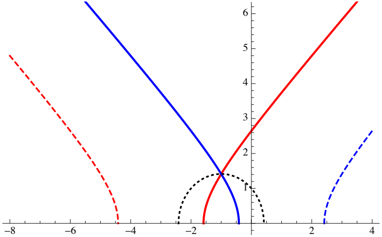

Large volume scattering diagram

- For the stability conditions $(Z^{LV_{(s,t)}}, \mathcal{A}(s))$, [Bousseau'19] constructed the scattering diagram $\mathcal{D}_\psi$ in (s,t) upper half-plane for $\psi = 0$. For $\psi \neq 0$, just map $(s,t) \mapsto (s - t\tan\psi, t/\cos\psi)$.
- The rays $\mathcal{R}(\gamma)$ are branches of hyperbola asymptoting to $t = \pm(s - \frac{d}{r})$ for $r \neq 0$, or vertical lines when $r = 0$. Walls of marginal stability $\mathcal{W}(\gamma, \gamma')$ are half-circles centered on real axis.

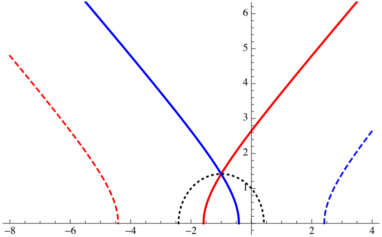

- Think of $\mathcal{R}(\gamma)$ as the worldline of a fictitious particle of charge r, mass $m^2 = \frac{1}{2}d^2 - r\,\mathrm{ch}_2$ moving in a constant electric field !

Large volume scattering diagram

- Initial rays correspond to $\mathcal{O}(m)$ and $\mathcal{O}(m)[1]$, *ie* (anti)D4-branes with m units of flux, emanating from $(s, t) = (m, 0)$ on the boundary where the central charge vanishes.

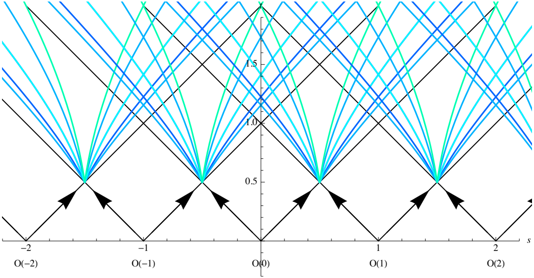

Large volume scattering diagram

- Initial rays correspond to $\mathcal{O}(m)$ and $\mathcal{O}(m)[1]$, *ie* (anti)D4-branes with m units of flux, emanating from $(s,t)=(m,0)$ on the boundary where the central charge vanishes.

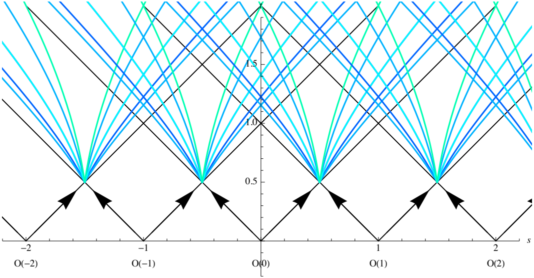

- The first scatterings occur for $t \geq \frac{1}{2}$, after each constituent has moved by $|\Delta s| \geq \frac{1}{2}$. Causality and monotonicity of the 'electric potential' $\varphi(\gamma) = d - sr$ along the flow, allow to bound the number and charges of constituents.

Flow trees for $\gamma = [0, 4, 1)$

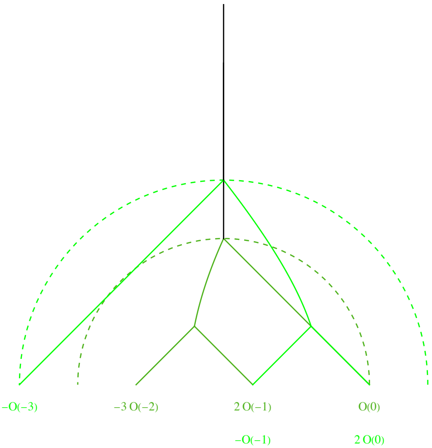

- $\{\{-3\mathcal{O}(-2), 2\mathcal{O}(-1)\}, \mathcal{O}\}$:
  $3\mathcal{O}(-2) \to 2\mathcal{O}(-1) \oplus \mathcal{O} \to E$
  $K_3(2,3) K_{12}(1,1) \to -156$

- $\{-\mathcal{O}(-3), \{-\mathcal{O}(-1), 2\mathcal{O}\}\}$:
  $\mathcal{O}(-3) \oplus \mathcal{O}(-1) \to 2\mathcal{O} \to E$
  $K_3(1,2) K_{12}(1,1) \to -36$

Total: $\Omega_\infty(\gamma) = -192 = GV_4^{(0)}$

Flow trees for $\gamma = [1, 0, -3)$

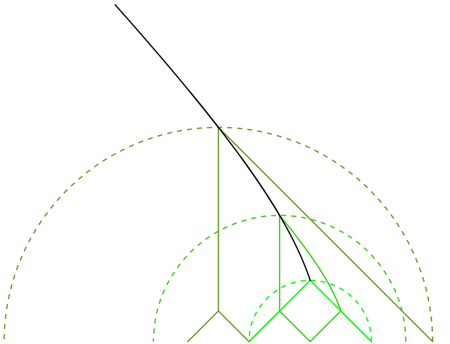

- $\{\{-\mathcal{O}(-5), \mathcal{O}(-4)\}, \mathcal{O}(-1)\}$
  $\mathcal{O}(-5) \to \mathcal{O}(-4) \oplus \mathcal{O}(-1) \to E$
  $K_3(1,1)^2 \to 9$
- $\{\{-\mathcal{O}(-4), \mathcal{O}(-3)\},$
  $\{-\mathcal{O}(-3), 2\mathcal{O}(-2)\}\}$
  $\mathcal{O}(-4) \oplus \mathcal{O}(-3) \to$
  $\mathcal{O}(-3) \oplus 2\mathcal{O}(-2) \to E$
  $K_3(1,1)^2 K_3(1,2) \to 27$
- $\{-\mathcal{O}(-4), 2\mathcal{O}(-2)\}$
  $\mathcal{O}(-4) \to 2\mathcal{O}(-2) \to E$
  $K_6(1,2) \to 15$

Total: $\Omega_\infty(\gamma) = 51 = \chi(\mathrm{Hilb}_4 \mathbb{P}^2)$

Outline

Exact scattering diagram

- The full scattering diagram $\mathcal{D}_\psi^\Pi$ on the slice of Π-stability conditions should interpolate between $\mathcal{D}_\psi^{\rm LV}$ around $\tau = \mathrm{i}\infty$ and $\mathcal{D}_\psi^o$ around $\tau = \frac{1}{\sqrt{3}} e^{\mathrm{i}\pi/6} + n$, and be invariant under the action of $\Gamma_1(3)$.

Exact scattering diagram

- The full scattering diagram $\mathcal{D}^{\Pi}_{\psi}$ on the slice of Π-stability conditions should interpolate between $\mathcal{D}^{\rm LV}_{\psi}$ around $\tau = \mathrm{i}\infty$ and $\mathcal{D}^{o}_{\psi}$ around $\tau = \frac{1}{\sqrt{3}} e^{\mathrm{i}\pi/6} + n$, and be invariant under the action of $\Gamma_1(3)$.
- Under $\tau \mapsto \frac{\tau}{3n\tau+1}$ with $n \in \mathbb{Z}$, $\mathcal{O} \mapsto \mathcal{O}[n]$. Hence we have an doubly infinite family of initial rays associated to $\mathcal{O}(m)[n]$.

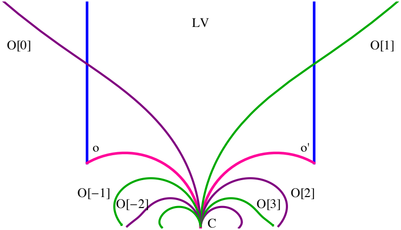

Exact scattering diagram

- The full scattering diagram $\mathcal{D}^{\Pi}_{\psi}$ on the slice of Π-stability conditions should interpolate between $\mathcal{D}^{\rm LV}_{\psi}$ around $\tau = i\infty$ and $\mathcal{D}^{o}_{\psi}$ around $\tau = \frac{1}{\sqrt{3}} e^{i\pi/6} + n$, and be invariant under the action of $\Gamma_1(3)$.
- Under $\tau \mapsto \frac{\tau}{3n\tau+1}$ with $n \in \mathbb{Z}$, $\mathcal{O} \mapsto \mathcal{O}[n]$. Hence we have an doubly infinite family of initial rays associated to $\mathcal{O}(m)[n]$.

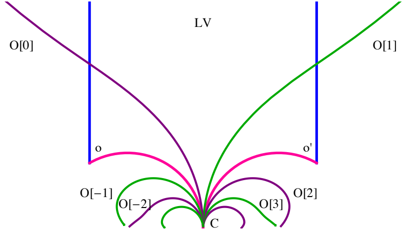

- For $|\tan\psi| < \frac{1}{2\mathcal{V}}$ where $\mathcal{V} = \mathrm{Im}\, T(0) = \frac{27}{4\pi^2} \mathrm{Im Li}_2(e^{2\pi i/3}) \simeq 0.463$ only the rays associated to $\mathcal{O}(m)[0]$ and $\mathcal{O}(m)[1]$ escape to $i\infty$, and merge onto rays in the large volume scattering diagram $\mathcal{D}^{\rm LV}_{\psi}$.

Exact scattering diagram

- In addition, there must be an infinite family of initial rays coming from $\tau = \frac{p}{q}$ with $q \neq 0 \mod 3$, corresponding to $\Gamma_1(3)$-images of $\mathcal{O}(0)$. This includes initial rays emitted at $\tau = n - \frac{1}{2}$, associated to $\Omega(n+1)$; for $\psi \sim \frac{\pi}{2}$, these merge onto initial rays of the orbifold scattering diagram.

Exact scattering diagram

- In addition, there must be an infinite family of initial rays coming from $\tau = \frac{p}{q}$ with $q \neq 0 \mod 3$, corresponding to $\Gamma_1(3)$-images of $\mathcal{O}(0)$. This includes initial rays emitted at $\tau = n - \frac{1}{2}$, associated to $\Omega(n+1)$; for $\psi \sim \frac{\pi}{2}$, these merge onto initial rays of the orbifold scattering diagram.
- Since $\partial_\tau Z(\gamma) = (d - r\tau)C(\tau)$ and $C \neq 0$ for $\mathrm{Im}\tau > 0$, it appears that rays $\mathcal{R}_\psi(\gamma)$ can only end at $\tau = \frac{d}{r}$ such that $Z_\tau(\gamma)$ vanishes. This can be shown to hold for generic ψ, but when $\mathcal{V} \tan \psi \in \mathbb{Q}$, a ray $\mathcal{R}(\gamma)$ emitted at $\tau = \frac{d}{r}$ might end up at $\tau' = \frac{d'}{r'}$ with $Z_{\tau'}(\gamma) \neq 0$.

Exact scattering diagram

- In addition, there must be an infinite family of initial rays coming from $\tau = \frac{p}{q}$ with $q \neq 0 \mod 3$, corresponding to $\Gamma_1(3)$-images of $\mathcal{O}(0)$. This includes initial rays emitted at $\tau = n - \frac{1}{2}$, associated to $\Omega(n+1)$; for $\psi \sim \frac{\pi}{2}$, these merge onto initial rays of the orbifold scattering diagram.
- Since $\partial_\tau Z(\gamma) = (d - r\tau)C(\tau)$ and $C \neq 0$ for $\mathrm{Im}\tau > 0$, it appears that rays $\mathcal{R}_\psi(\gamma)$ can only end at $\tau = \frac{d}{r}$ such that $Z_\tau(\gamma)$ vanishes. This can be shown to hold for generic ψ, but when $\mathcal{V} \tan\psi \in \mathbb{Q}$, a ray $\mathcal{R}(\gamma)$ emitted at $\tau = \frac{d}{r}$ might end up at $\tau' = \frac{d'}{r'}$ with $Z_{\tau'}(\gamma) \neq 0$.
- We conjecture that the only initial rays are the $\Gamma_1(3)$ images of the structure sheaf $\mathcal{O}$, each of them carrying $\Omega(k\gamma) = 1$ for $k = 1$, 0 otherwise.

Exact scattering diagram - $\psi = 0$

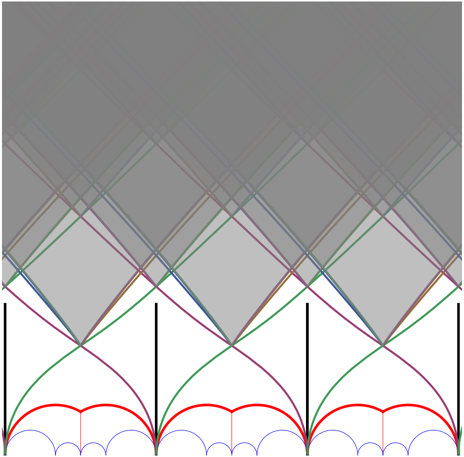

Exact scattering diagram - $\psi = \pm\frac{\pi}{2} \mod 2\pi$

- For $\psi = \pm\frac{\pi}{2}$, the diagram $\mathcal{D}^{\Pi}_{\psi}$ simplifies dramatically, since the loci $\mathrm{Im}Z_{\tau}(\gamma) = 0$ are lines of constant $s := \frac{\mathrm{Im}\, T_D}{\mathrm{Im}\, T} = \frac{d}{r}$.

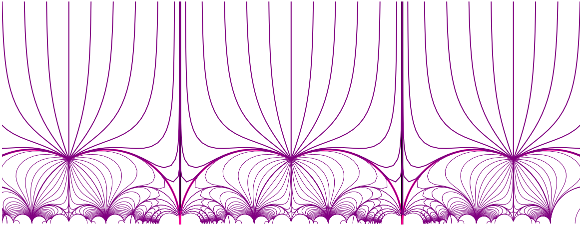

Exact scattering diagram - $\psi = \pm\frac{\pi}{2} \mod 2\pi$

- For $\psi = \pm\frac{\pi}{2}$, the diagram $\mathcal{D}^{\Pi}_{\psi}$ simplifies dramatically, since the loci $\mathrm{Im} Z_\tau(\gamma) = 0$ are lines of constant $s := \frac{\mathrm{Im}\, T_D}{\mathrm{Im}\, T} = \frac{d}{r}$.

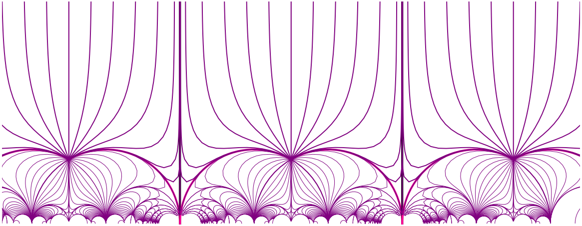

- Hence, there is no wall-crossing between τ_o and $\tau = \mathrm{i}\infty$ when $-1 \leq \frac{d}{r} \leq 0$, explaining why the Gieseker index $\Omega_\infty(\gamma)$ agrees with the index $\Omega_{-\zeta_*(\gamma)}(\gamma)$ in the anti-attractor chamber. In that chamber, the orbifold quiver with potential reduces to the Beilinson quiver with relations *[Douglas Fiol Romelsberger'00]*

Scattering diagram in affine coordinates

- For $|\tan\psi| < \frac{1}{2\mathcal{V}}$ and fixed γ, the flow trees in $\mathcal{D}_\psi^\Pi$ are identical (topologically) to flow trees in $\mathcal{D}_\psi^{\rm LV}$. One way to show this is to map both of them to the plane

$$x = \frac{\mathrm{Re}\left(e^{-\mathrm{i}\psi} T\right)}{\cos\psi}\,, \quad y = -\frac{\mathrm{Re}\left(e^{-\mathrm{i}\psi} T_D\right)}{\cos\psi}\,,$$

such that $\mathcal{R}_\psi(\gamma)$ becomes a line segment $rx + dy - \mathrm{ch}_2 = 0$.

Scattering diagram in affine coordinates

- For $|\tan\psi| < \frac{1}{2\mathcal{V}}$ and fixed γ, the flow trees in $\mathcal{D}_\psi^\Pi$ are identical (topologically) to flow trees in $\mathcal{D}_\psi^{\rm LV}$. One way to show this is to map both of them to the plane

$$x = \frac{\mathrm{Re}\left(e^{-\mathrm{i}\psi} T\right)}{\cos\psi} , \quad y = -\frac{\mathrm{Re}\left(e^{-\mathrm{i}\psi} T_D\right)}{\cos\psi} ,$$

such that $\mathcal{R}_\psi(\gamma)$ becomes a line segment $rx + dy - \mathrm{ch}_2 = 0$.

- The initial rays $\mathcal{R}_{\mathcal{O}(m)}$ are tangent to the parabola $y = -\frac{1}{2}x^2$ at $x = m$, but the origin of each ray is shifted to $x = m + \mathcal{V}\tan\psi$.

Scattering diagram in affine coordinates

- For $|\tan\psi| < \frac{1}{2\mathcal{V}}$ and fixed γ, the flow trees in $\mathcal{D}^{\Pi}_{\psi}$ are identical (topologically) to flow trees in $\mathcal{D}^{\rm LV}_{\psi}$. One way to show this is to map both of them to the plane

$$x = \frac{\mathrm{Re}\left(e^{-\mathrm{i}\psi} T\right)}{\cos\psi}\ , \quad y = -\frac{\mathrm{Re}\left(e^{-\mathrm{i}\psi} T_D\right)}{\cos\psi}\ ,$$

  such that $\mathcal{R}_{\psi}(\gamma)$ becomes a line segment $rx + dy - \mathrm{ch}_2 = 0$.
- The initial rays $\mathcal{R}_{\mathcal{O}(m)}$ are tangent to the parabola $y = -\frac{1}{2}x^2$ at $x = m$, but the origin of each ray is shifted to $x = m + \mathcal{V}\tan\psi$.
- In addition, there are initial rays associated to images of $\mathcal{O}(m)$ under $\Gamma_1(3)$, but those don't play a role if ψ is small enough.

Exact scattering diagram in (x, y) plane, $\psi = 1$

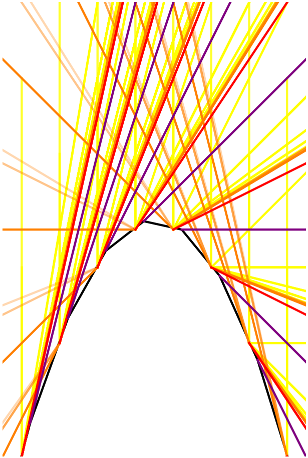

Exact scattering diagram, varying ψ

$\gamma = [0, 1, 1) = \mathrm{ch}\,\mathcal{O}_C$:

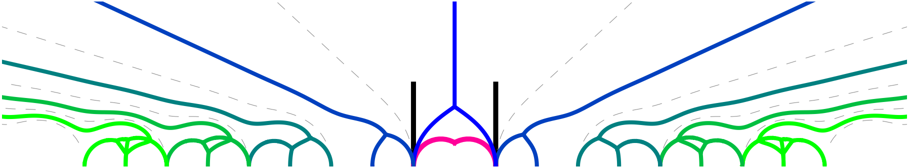

$\gamma = [1, 0, 1) = \mathrm{ch}\,\mathcal{O}$:

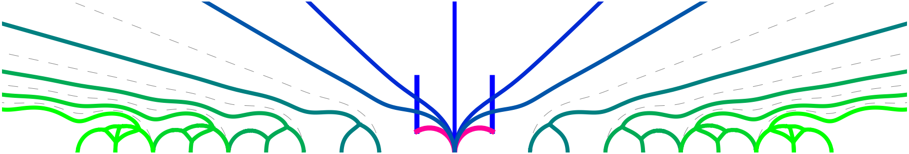

Conclusion - outlook

- The scattering diagram is the proper mathematical framework for the attractor flow tree formula in the case of local CY3. This is because the central charge is holomorphic, so the gradient flow preserves the phase of $Z(\gamma)$. Moreover, initial rays can only start from the boundary.

Conclusion - outlook

- The scattering diagram is the proper mathematical framework for the attractor flow tree formula in the case of local CY3. This is because the central charge is holomorphic, so the gradient flow preserves the phase of $Z(\gamma)$. Moreover, initial rays can only start from the boundary.
- This provides an effective way of computing (unframed) BPS invariants in any chamber, and a natural decomposition into elementary constituents. Mathematically, different trees should correspond to different strata in $\mathcal{M}_Z(\gamma)$, but the precise relation is not clear.

Conclusion - outlook

- The scattering diagram is the proper mathematical framework for the attractor flow tree formula in the case of local CY3. This is because the central charge is holomorphic, so the gradient flow preserves the phase of $Z(\gamma)$. Moreover, initial rays can only start from the boundary.
- This provides an effective way of computing (unframed) BPS invariants in any chamber, and a natural decomposition into elementary constituents. Mathematically, different trees should correspond to different strata in $\mathcal{M}_Z(\gamma)$, but the precise relation is not clear.
- It would be interesting to extend this description to other toric CY3, such as local del Pezzo surfaces, and to framed BPS indices.

Conclusion - outlook

- The scattering diagram is the proper mathematical framework for the attractor flow tree formula in the case of local CY3. This is because the central charge is holomorphic, so the gradient flow preserves the phase of $Z(\gamma)$. Moreover, initial rays can only start from the boundary.
- This provides an effective way of computing (unframed) BPS invariants in any chamber, and a natural decomposition into elementary constituents. Mathematically, different trees should correspond to different strata in $\mathcal{M}_Z(\gamma)$, but the precise relation is not clear.
- It would be interesting to extend this description to other toric CY3, such as local del Pezzo surfaces, and to framed BPS indices.
- In the compact case, $\arg Z(\gamma)$ is no longer constant along the flow and there can be attractor points with $\Omega_\star(\gamma) \neq 0$ at finite distance in Kähler moduli space...

Thanks for your attention !